SUPPLEMENTARY INFORMATION

S1. Quantifying glassy rearrangements

Using the trajectories generated for softness, we first choose a rearrangement timescale t_R over which to evaluate the indicator function p_{hop}. Recall that the time intervals before (A) and after (B) a rearrangement event are given by,

$A = [t - t_R/2, t]$	(25)
$B = [t, t_R/2]$	(26)

and that the indicator function for the i^{th} particle is defined as,

$p_{hop}(i,t) = \sqrt{\langle \lvert r_i(t) - \langle r_i \rangle_B \rvert^2 \rangle_A \langle \lvert r_i(t) - \langle r_i \rangle_A \rvert^2 \rangle_B}$	(27)

where i is the particle index, $r_i(t)$ is its position at time t, and the angle bracketed quantities $\langle\,\rangle_A$ and $\langle\,\rangle_B$ are averages over the time intervals A and B.We identify a critical value $p_{cut,R} = 0.25$, constant across all systems, that indicates a particle has undergone a rearrangement of at least $0.5\,\sigma$ in that time. The choice of this value is motivated below.

To visualize the magnitude of the rearrangements in our system, we use an approach that takes advantage of the ease with which we can do single-particle-tracking in a simulation[52]. Following the value of a particle's p_{hop} as a function of time, we note when it surpasses the threshold $p_{cut,R}$. The position of the particle is recorded as r_1 at time t_1, and we continue to monitor it until it falls below $p_{cut,R}$ again. At this point, we record the position and time again, r_2 and t_2, and say that the particle has undergone an "event", noting the maximum value of p_{hop} achieved during the event, p_{hop}^*. The magnitudes of the event in size and time are,

$\lvert \Delta r \rvert = \lvert r_2 - r_1 \rvert$	(28)
$\Delta t = t_2 - t_1$	(29)

and one can plot the $\langle \lvert \Delta r \rvert \rangle$ and $\langle \Delta t \rangle$ values as a function of p_{hop}^*.

We first identify that, for a constant value of the rearrangement time $t_R = 10\,\tau$, there is a scaling of the size of an event observed $\lvert \Delta r \rvert \sim {p_{hop}^*}^{1/2}$ which is invariant in temperature so long as the event threshold $p_{cut,R}$ is large enough. Intuitively, this makes sense: in the limiting case of a rearrangement at time t^* where there is a discrete jump between r_1 and r_2 such that $\langle r \rangle_A = r_1$ and $\langle r \rangle_B = r_2$ with zero variance, Equation (27) becomes,

$p_{hop}^* = \sqrt{\lvert r_2 - r_1 \rvert^4} = \lvert \Delta r \rvert^2$	(30)

which is equivalent to the relationship identified above. We make the helpful observation that, for different particle sizes σ_{BB} and rearrangement cutoffs $p_{cut,R}$, plots of $\langle \lvert \Delta r \rvert \rangle$ versus p_{hop}^* normalized by the length scale $\sqrt{p_{cut,R}}$ collapse onto one another with the limiting behavior,

$\lim_{\left(\frac{p_{hop}^*}{p_{cut,R}}\right)\to 1} \left(\frac{\langle \lvert \Delta r \rvert \rangle}{\sqrt{p_{cut}}}\right) = 0$	(31)
$\lim_{\left(\frac{p_{hop}^*}{p_{cut,R}}\right)\to \infty} \left(\frac{\langle \lvert \Delta r \rvert \rangle}{\sqrt{p_{cut}}}\right) = \left(\frac{p_{hop}^*}{p_{cut,R}}\right)^{1/2}$	(32)

across all investigated particle sizes, rearrangement cutoffs, and temperatures. This finding motivates the use of the same displacement cutoff $p_{cut,R}$ in comparing rearrangements of the same absolute size across systems.

A final note on the scaling of $\langle \lvert \Delta r \rvert \rangle$ with p_{hop}^* is that if the normalizing length scale is instead chosen to be σ_{BB}, or the size of the particle of interest, the limits are then,

$\lim_{\left(\frac{p_{hop}^*}{\sigma_{BB}^2}\right)\to\left(\frac{p_{cut,R}}{\sigma_{BB}^2}\right)} \left(\frac{\langle \lvert \Delta r \rvert \rangle}{\sigma_{BB}}\right) = 0$	(33)
$\lim_{\left(\frac{p_{hop}^*}{\sigma_{BB}^2}\right)\to\infty} \left(\frac{\langle \lvert \Delta r \rvert \rangle}{\sigma_{BB}}\right) = \left(\frac{p_{hop}^*}{\sigma_{BB}^2}\right)^{1/2}$	(34)

which remains invariant in T but changes with σ_{BB} and $p_{cut,R}$. If a particle rearrangement is defined in terms of σ_{BB}, for example if $\left(\frac{\langle \lvert \Delta r \rvert \rangle}{\sigma_{BB}}\right) > d_p$, where d_p is the number of particle diameters, then this corresponds to $\left(\frac{p_{hop}^*}{\sigma_{BB}^2}\right) > d_p^2$. It is a necessity to have $\left(\frac{p_{cut}}{\sigma_{BB}^2}\right) < \left(\frac{p_{hop}^*}{\sigma_{BB}^2}\right)$, so $\left(\frac{p_{cut}}{\sigma_{BB}^2}\right) < d_p^2$ and,

$p_{cut} < (d_p \sigma_{BB})^2$	(35)

which is a maximum threshold for rearrangement detection.

In this work we consider all rearrangements to be at least size $0.5\ \sigma$; for an equivalent size relative to a small particle $d_p = 0.5$, we have $p_{cut} < 0.25\sigma_{BB}^2$. For our smallest particles of $\sigma_{BB} = 0.3$ this would mean $p_{cut} < 0.0225$. This is well within the threshold of what can be considered "thermal noise" in most systems and would make identifying individual rearranging motions nearly impossible. One possible solution would be to shorten t_R until the distribution of p_{hop} values has a lower mean value, but it may be better to seek some alternative indicator function in this case.

S2. Tracer diffusion and relaxation behavior

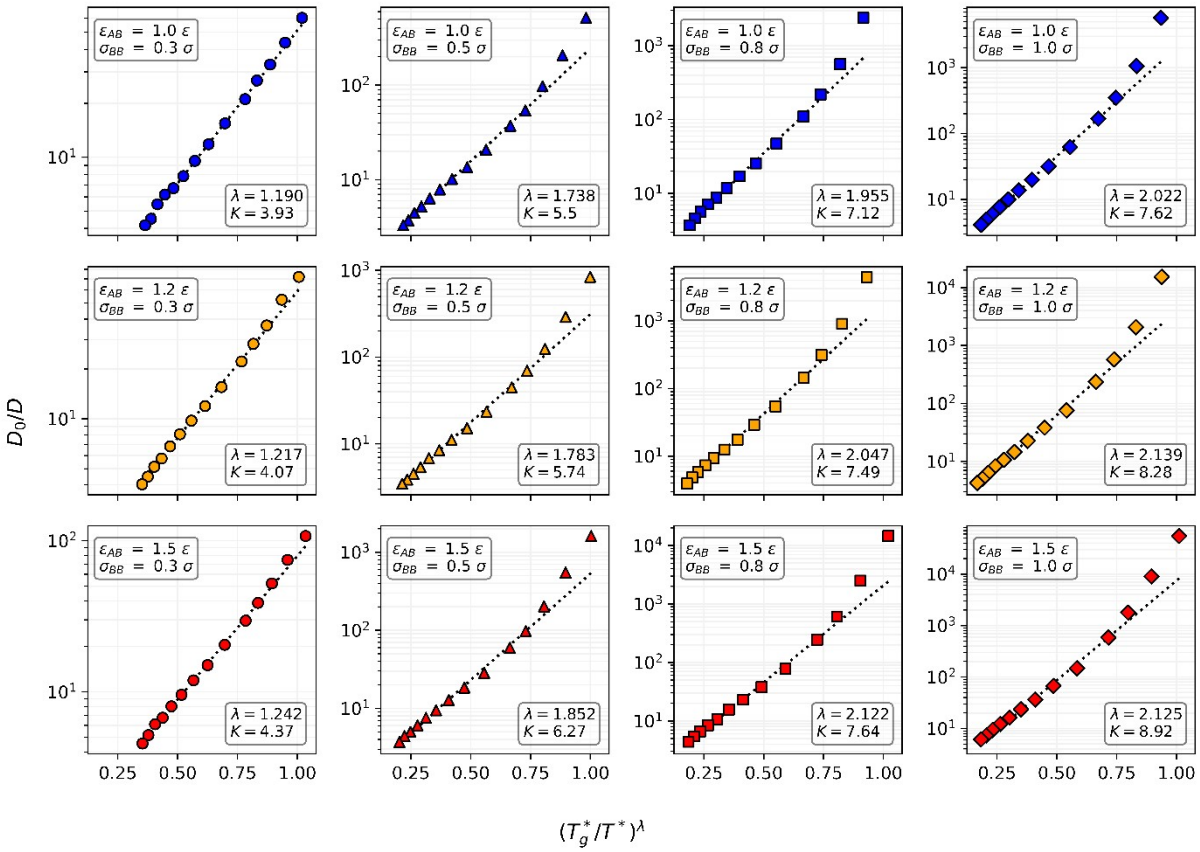

Figure S2.1. Inverse power-law fits of the reduced diffusion coefficient against T_g^*/T^* *across all systems studied. Fit parameters for the expression* $\log(D_0/D) = K(T_g^*/T^*)^\lambda$ *are indicated on each panel, as is the line of the function fitting the data just above the glass transition region* $(0.45 \leq T^* \leq 0.75)$.

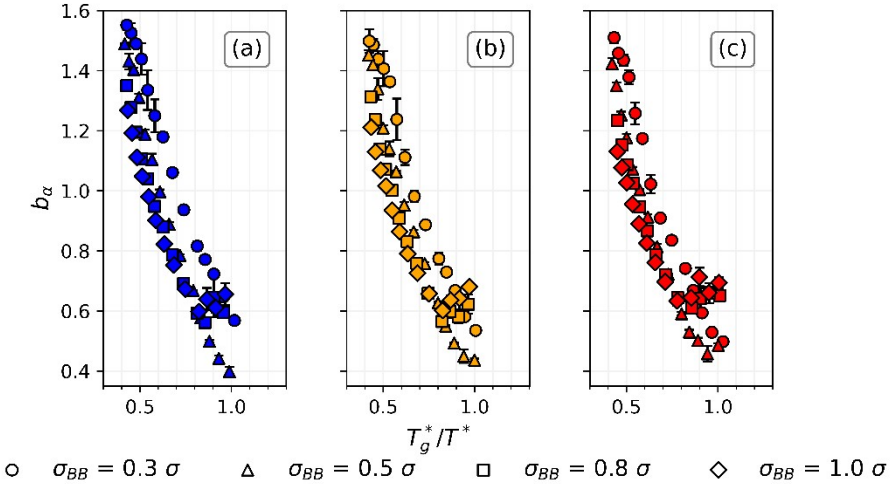

Figure S2.2 KWW stretching exponents b_α *for tracer molecules as a function of* T_g^*/T^*. *Symbols indicate* σ_{BB}, *while subplots indicate* ε_{AB} *values of (a)* $1.0\ \varepsilon$, *(b)* $1.2\ \varepsilon$, *and (c)* $1.5\ \varepsilon$.

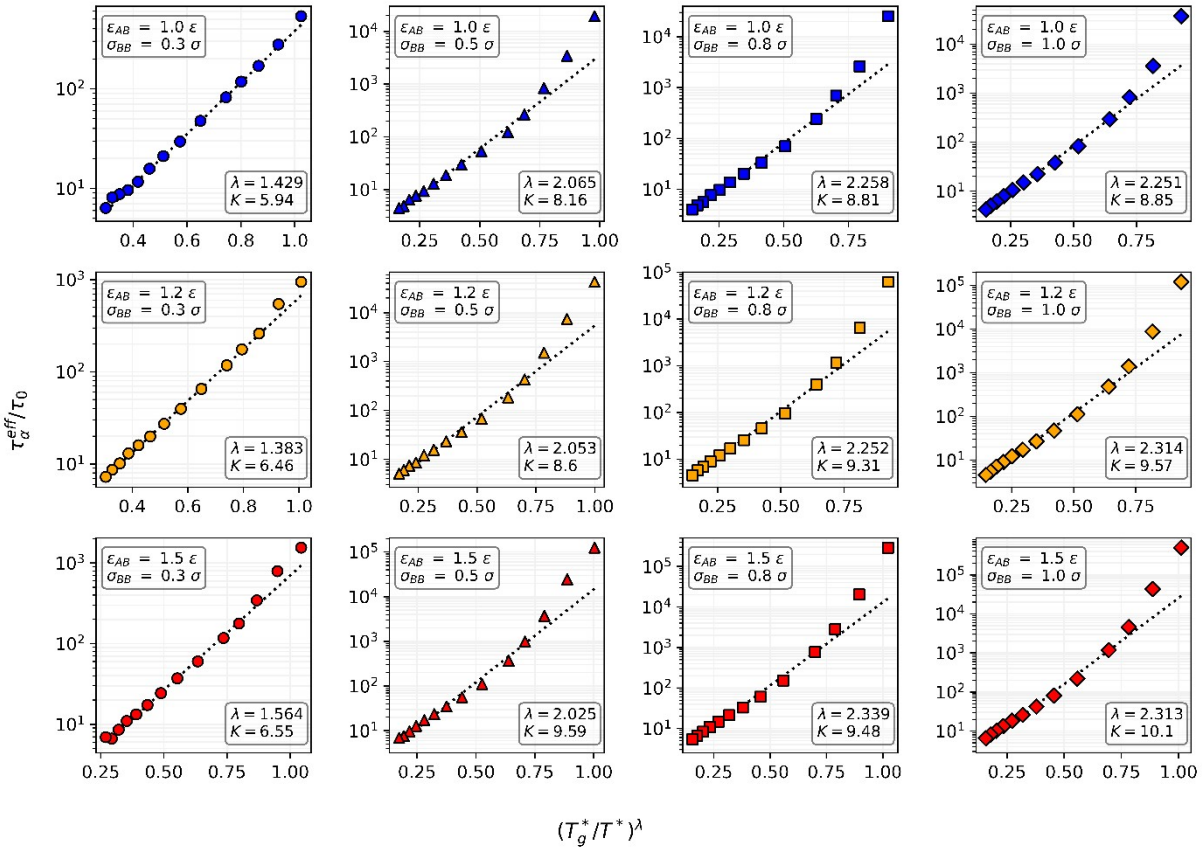

Figure S2.3. Inverse power-law fits of the reduced effective alpha relaxation time against T_g^*/T^* *across all systems studied. Fit parameters for the expression* $\log\left(\tau_\alpha^{eff}/\tau_0\right) = K\left(T_g^*/T^*\right)^\lambda$ *are indicated on each panel, as is the line of the function fitting the data just above the glass transition region* $(0.45 \le T^* \le 0.75)$.

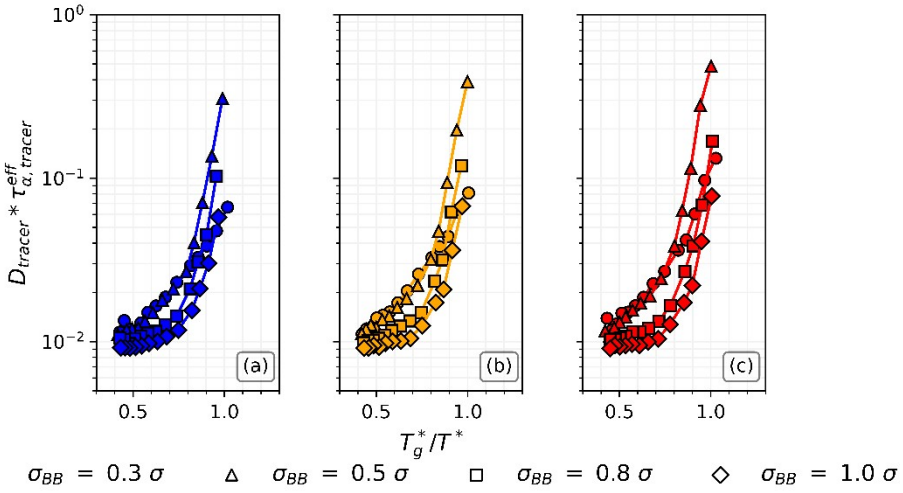

Figure S2.4. Ratio of tracer-tracer decoupling factors plotted against T_g^*/T^*. *Symbols indicate* σ_{BB}, *while subplots indicate* ε_{AB} *values of (a)* $1.0\ \varepsilon$, *(b)* $1.2\ \varepsilon$, *and (c)* $1.5\ \varepsilon$.

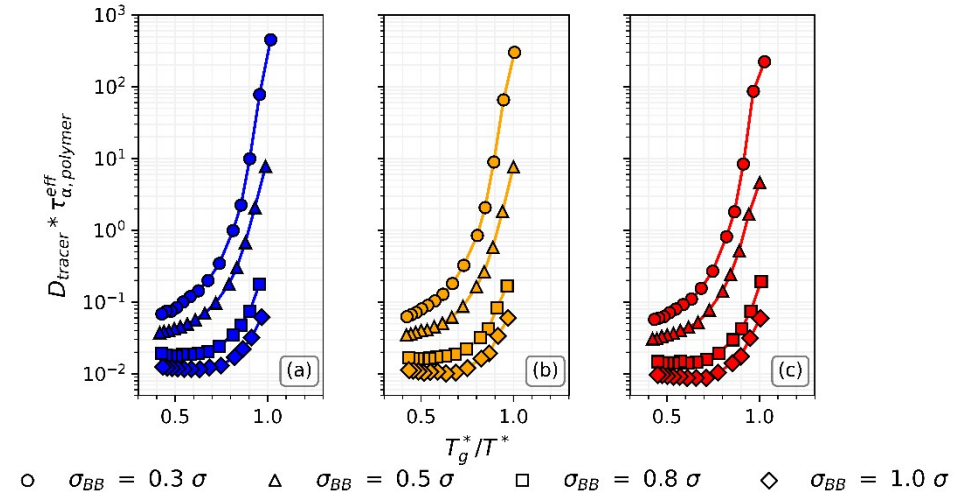

Figure S2.5. Ratio of tracer-polymer decoupling factors plotted against T_g^*/T^*. *Symbols indicate* σ_{BB}, *while subplots indicate* ε_{AB} *values of (a)* $1.0\ \varepsilon$, *(b)* $1.2\ \varepsilon$, *and (c)* $1.5\ \varepsilon$.

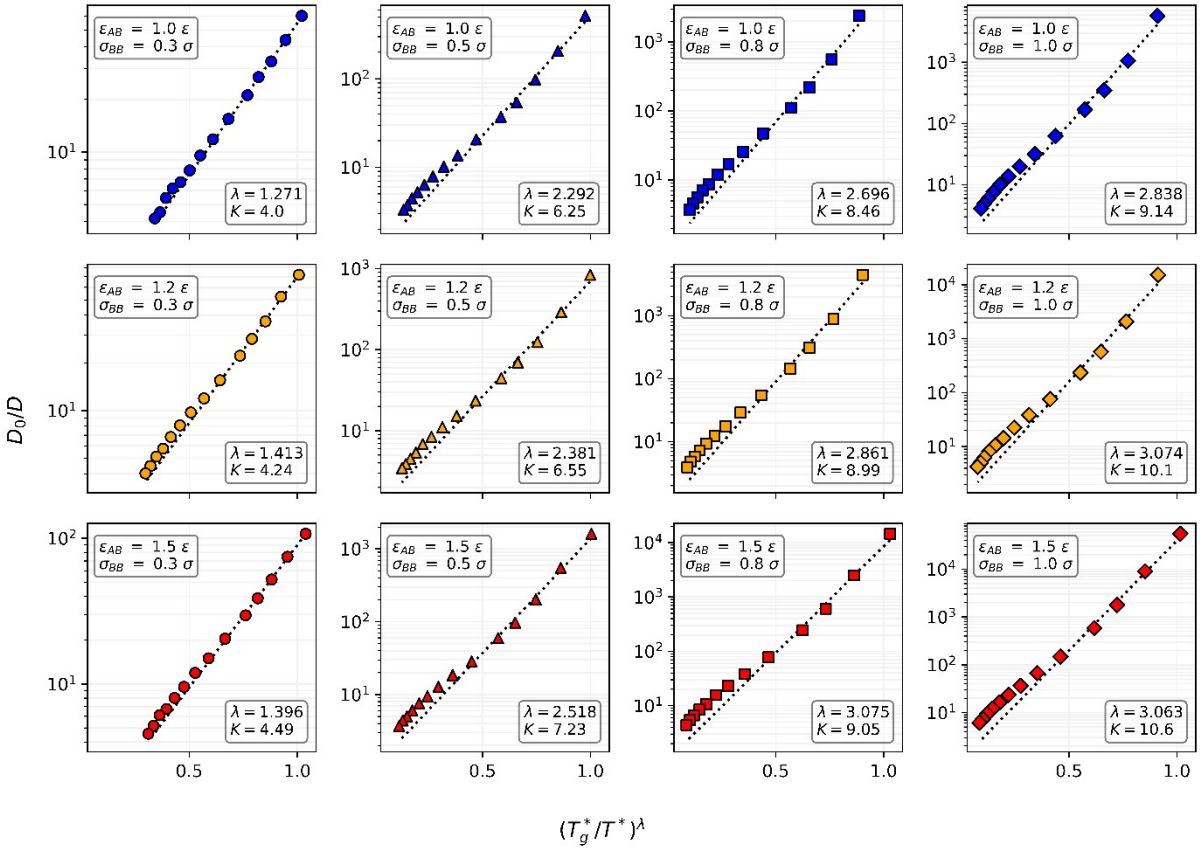

Figure S2 6. Low-temperature inverse power-law fits of the reduced diffusion coefficient against T_g^*/T^* *across all systems studied. Fit parameters for the expression* $\log(D_0/D) = K(T_g^*/T^*)^\lambda$ *are indicated on each panel, as is the line of the function fitting the data in the near-glass-transition region* $(0.40 \le T^* \le 0.55)$.

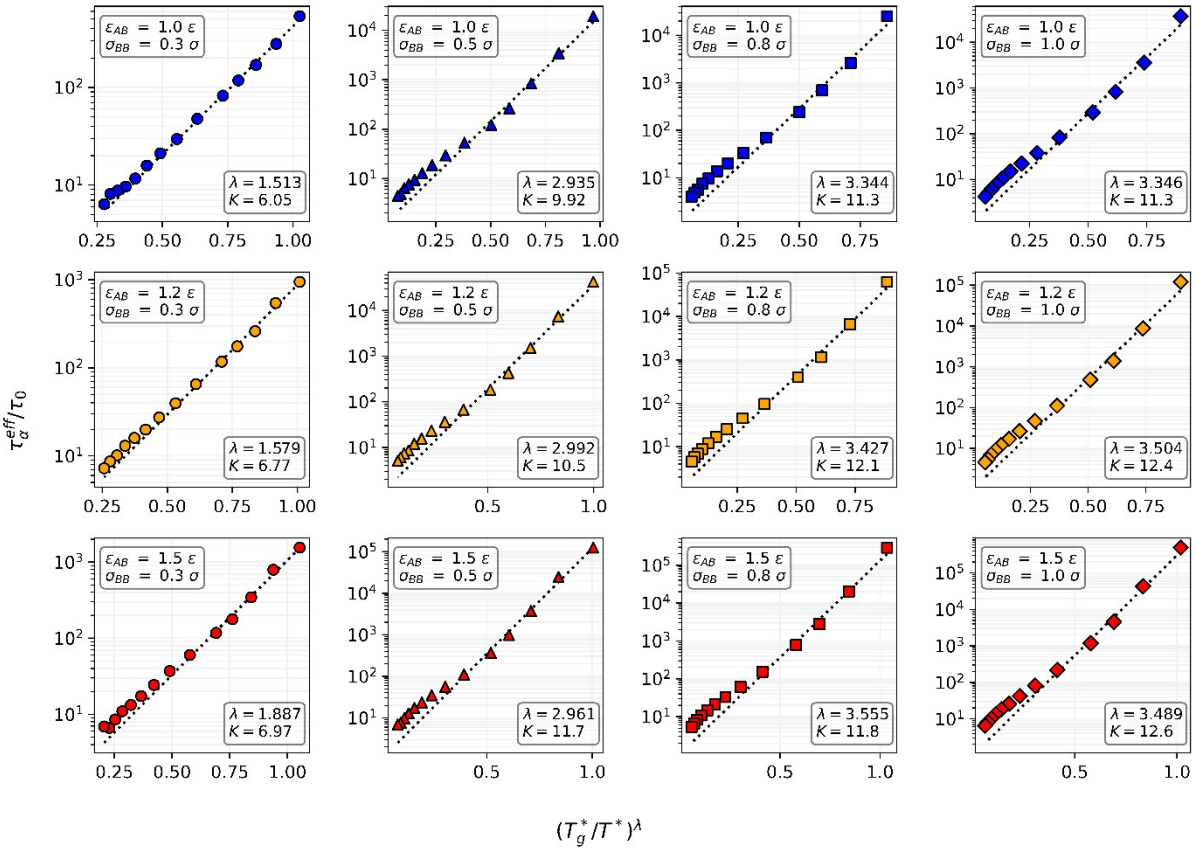

Figure S2 7. Low-temperature inverse power-law fits of the reduced effective alpha relaxation time against T_g^*/T^* *across all systems studied. Fit parameters for the expression* $\log\left(\tau_\alpha^{eff}/\tau_0\right) = K\left(T_g^*/T^*\right)^\lambda$ *are indicated on each panel, as is the line of the function fitting the data in the near-glass-transition region* $\left(0.40 \le T^* \le 0.55\right)$.

S3. Sensitivity analysis of hyperplane accuracy to $p_{cut,R}$ and $p_{cut,NR}$

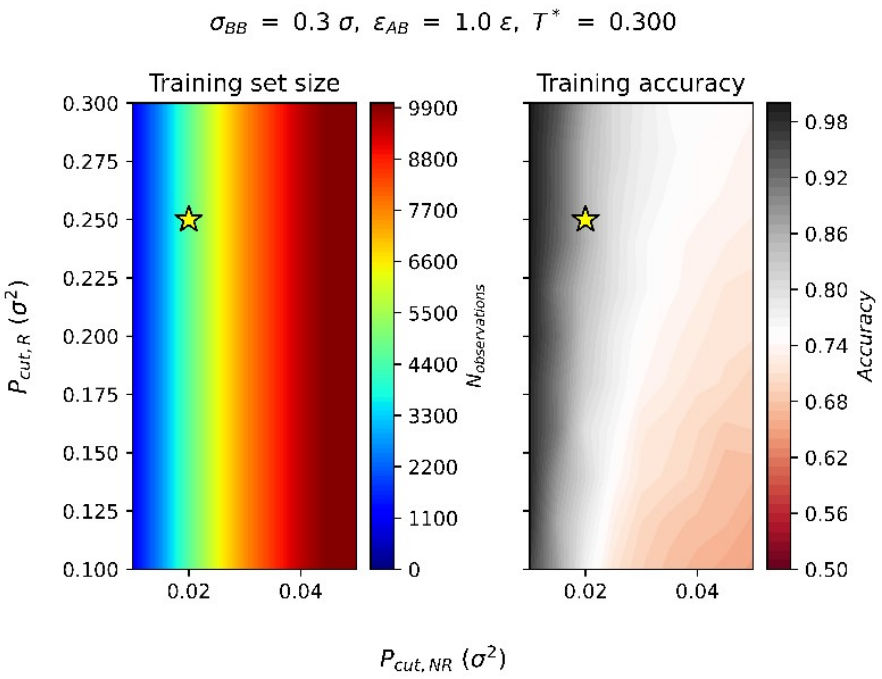

Figure S3.1. Sensitivity of sample size and accuracy A to the rearrangement and non-rearrangement cutoff parameters $p_{cut,R}$ and $p_{cut,NR}$ when training hyperplanes for the $\sigma_{BB} = 0.3\ \sigma$ and $\varepsilon_{AB} = 1.0\ \varepsilon$ system at $T^* = 0.300$ using $t_R = 10\ \tau$ and $t_{NR} = 10\ \tau$.

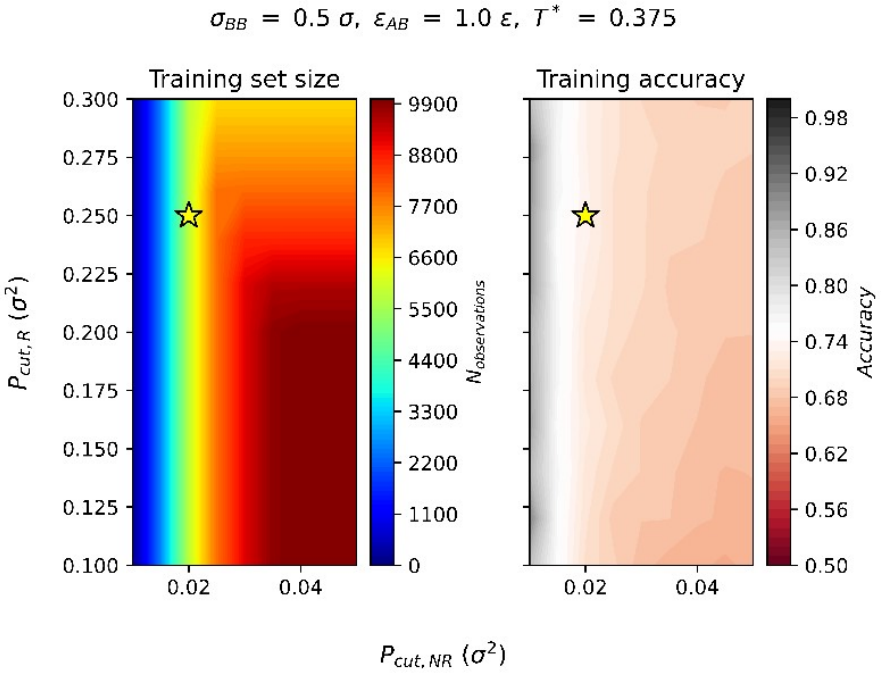

Figure S3.2. Sensitivity of sample size and accuracy A to the rearrangement and non-rearrangement cutoff parameters $p_{cut,R}$ and $p_{cut,NR}$ when training hyperplanes for the $\sigma_{BB} = 0.5\ \sigma$ and $\varepsilon_{AB} = 1.0\ \varepsilon$ system at $T^* = 0.375$ using $t_R = 10\ \tau$ and $t_{NR} = 10\ \tau$.

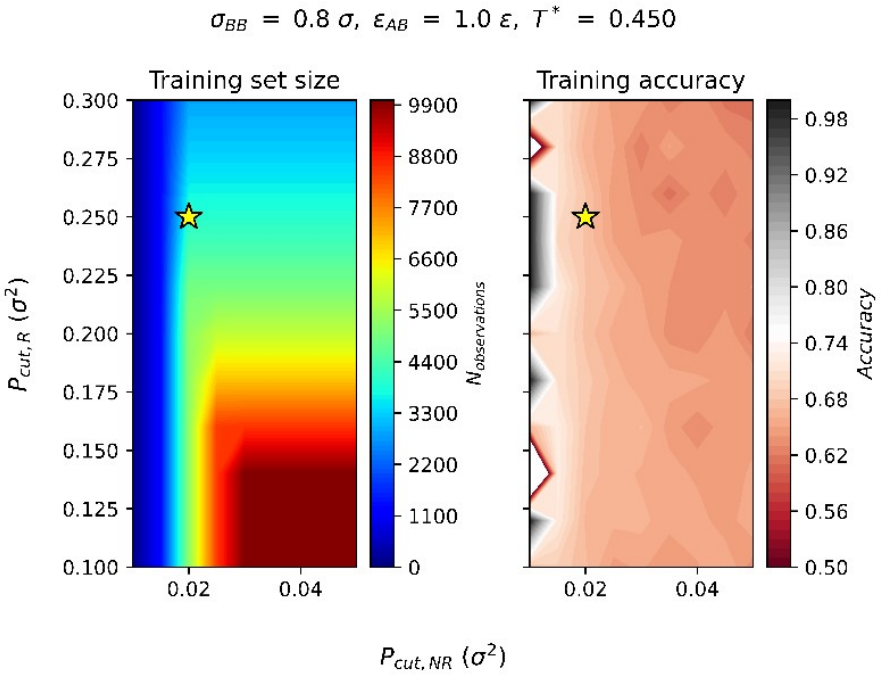

Figure S3.3. Sensitivity of sample size and accuracy A to the rearrangement and non-rearrangement cutoff parameters $p_{cut,R}$ and $p_{cut,NR}$ when training hyperplanes for the $\sigma_{BB} = 0.8\ \sigma$ and $\varepsilon_{AB} = 1.0\ \varepsilon$ system at $T^* = 0.450$ using $t_R = 10\ \tau$ and $t_{NR} = 10\ \tau$.

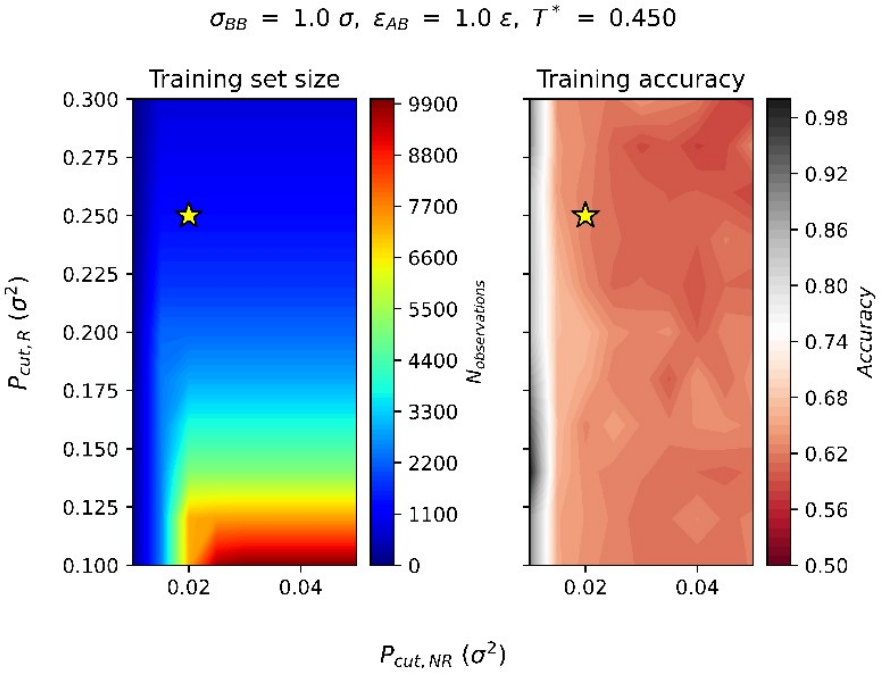

Figure S3.4. Sensitivity of sample size and accuracy A to the rearrangement and non-rearrangement cutoff parameters $p_{cut,R}$ and $p_{cut,NR}$ when training hyperplanes for the $\sigma_{BB} = 1.0\ \sigma$ and $\varepsilon_{AB} = 1.0\ \varepsilon$ system at $T^* = 0.450$ using $t_R = 10\ \tau$ and $t_{NR} = 10\ \tau$.

S4. Tracer softness training histograms and Arrhenius plots for different systems

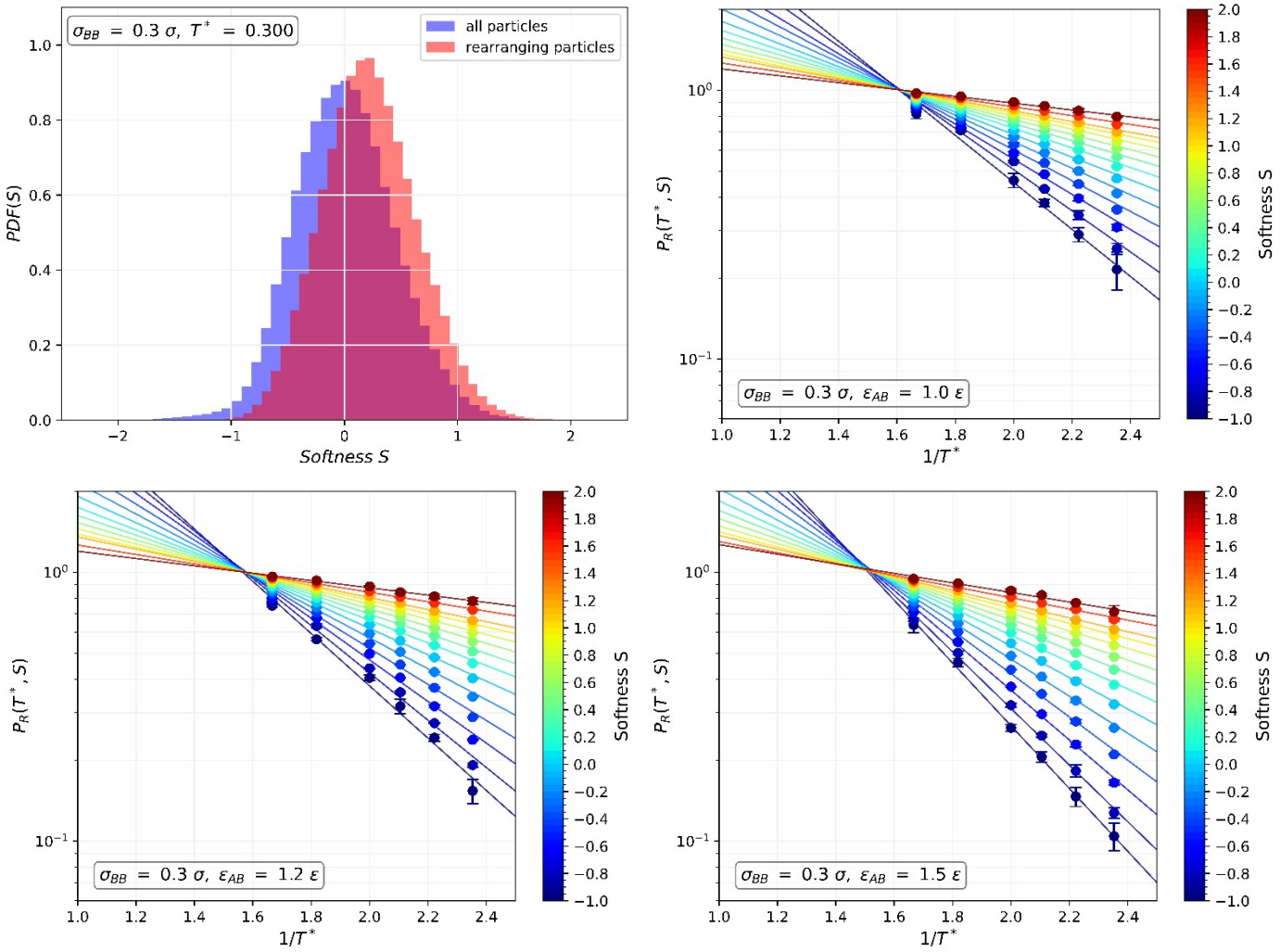

Figure S4.1. Training data histograms for the hyperplane trained on $\sigma_{BB} = 0.3\ \sigma$ *and* $\varepsilon_{AB} = 1.0\ \varepsilon$*, and Arrhenius decomposition plots of softness calculated for the differing values of* ε_{AB}*, indicated on subplots.*

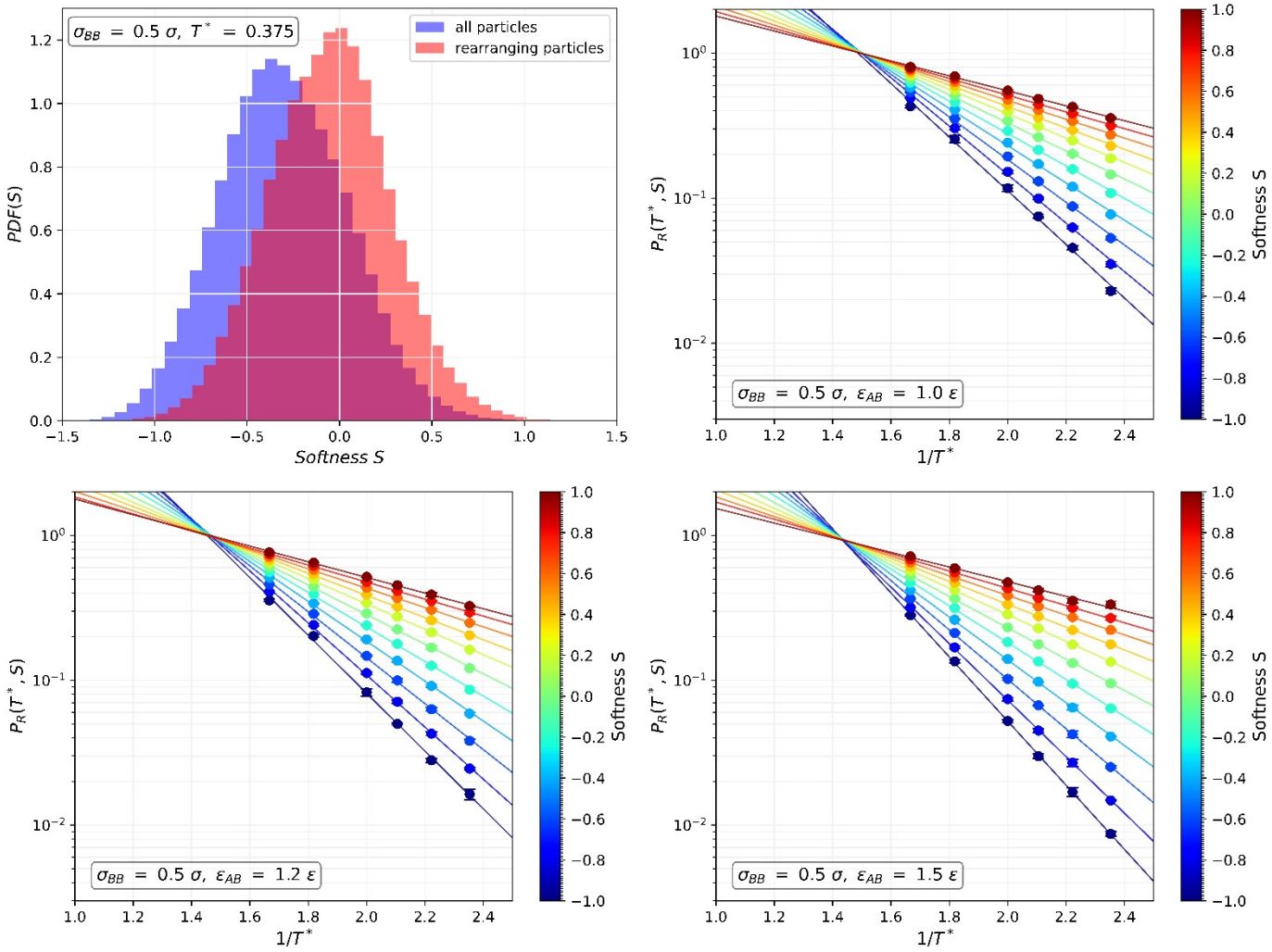

Figure S4.2. Training data histograms for the hyperplane trained on $\sigma_{BB} = 0.5\,\sigma$ *and* $\varepsilon_{AB} = 1.0\,\varepsilon$*, and Arrhenius decomposition plots of softness calculated for the differing values of* ε_{AB}*, indicated on subplots.*

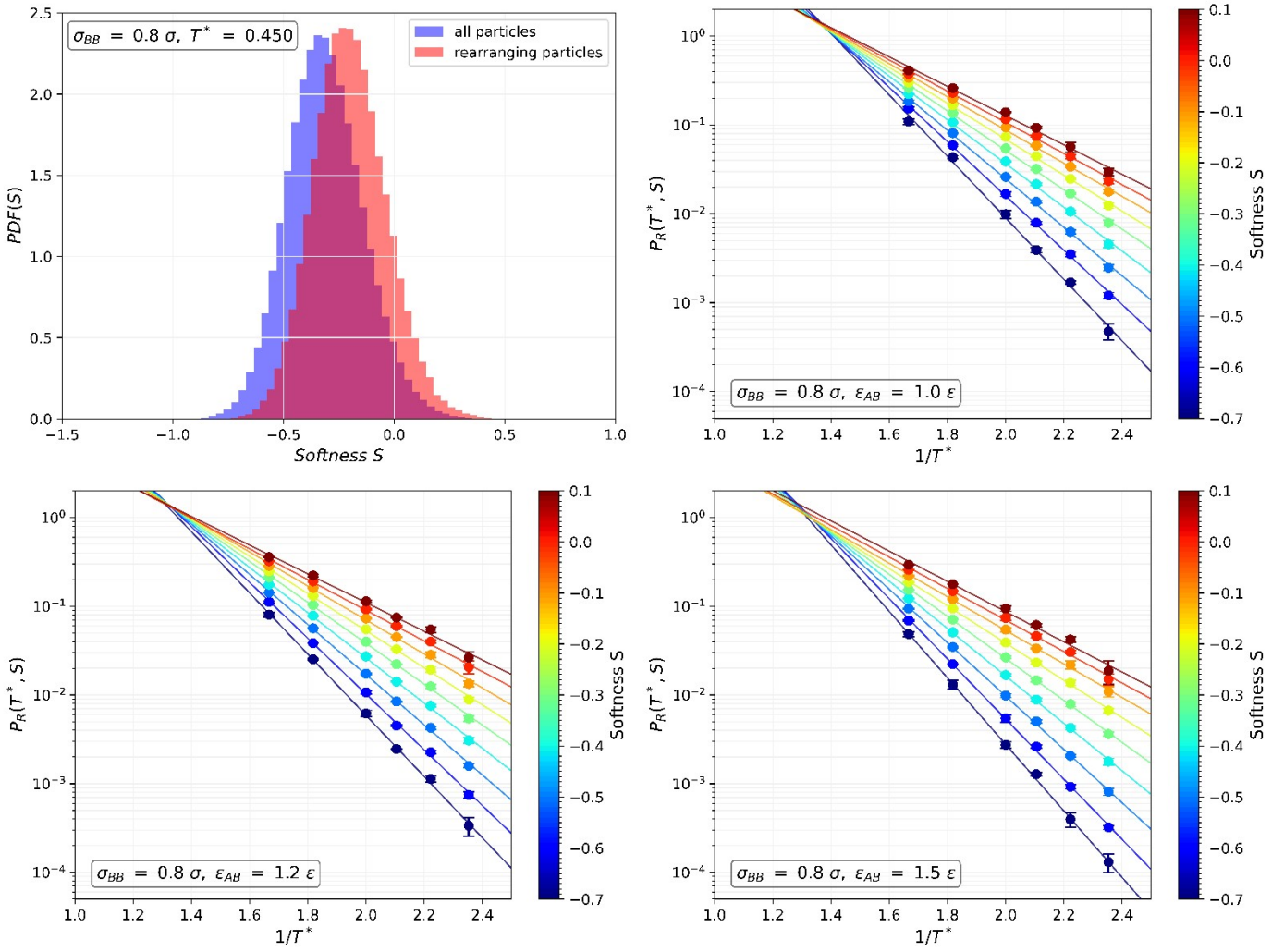

Figure S4.3. Training data histograms for the hyperplane trained on $\sigma_{BB} = 0.8\,\sigma$ *and* $\varepsilon_{AB} = 1.0\,\varepsilon$*, and Arrhenius decomposition plots of softness calculated for the differing values of* ε_{AB}*, indicated on subplots.*

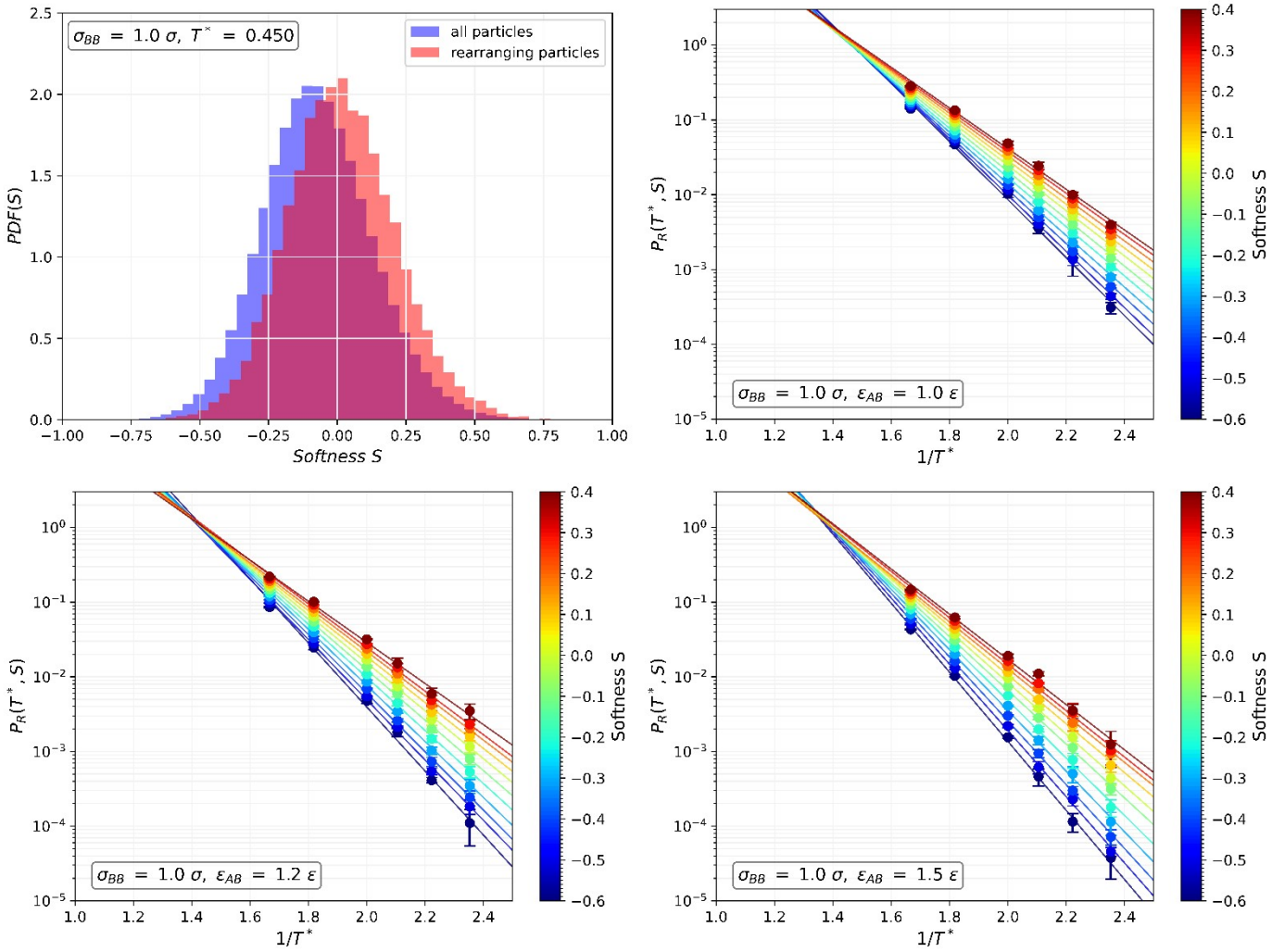

Figure S4.4. Training data histograms for the hyperplane trained on $\sigma_{BB} = 1.0\ \sigma$ *and* $\varepsilon_{AB} = 1.0\ \varepsilon$*, and Arrhenius decomposition plots of softness calculated for the differing values of* ε_{AB}*, indicated on subplots.*

S5. Impact of changing rearrangement cutoff parameter in softness analysis

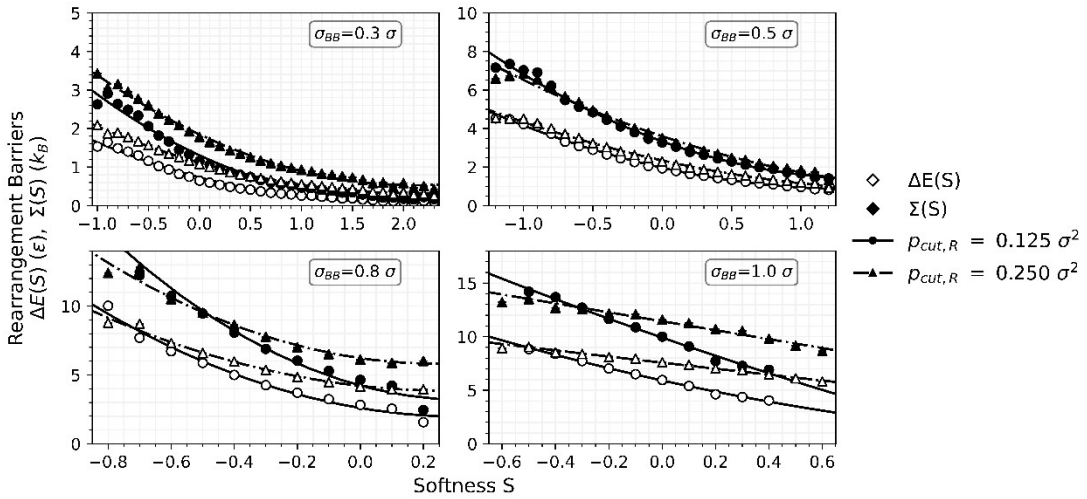

Figure S5.1. Comparison of energetic and entropic barriers to softness calculated using $p_{cut,R} = 0.25$ *and* $p_{cut,R} = 0.125$ *for systems with* $\varepsilon_{AB} = 1.0\ \varepsilon$ *as a function of softness, analogous to Figure 12 in the main text.*

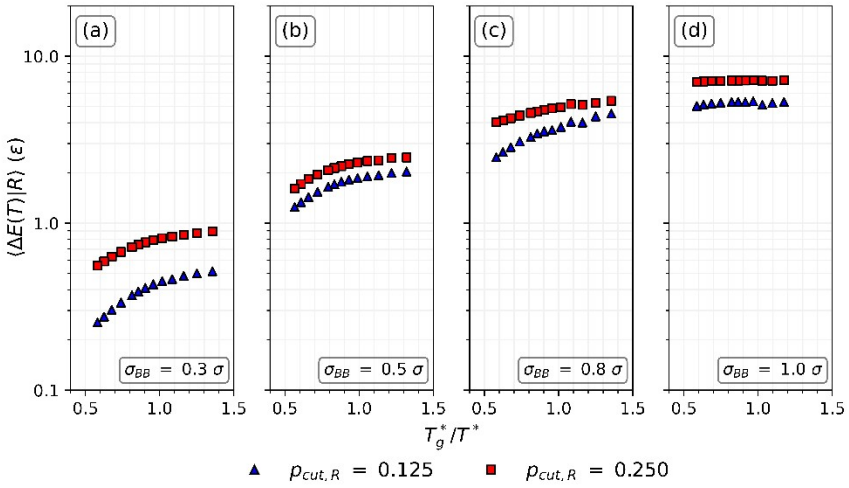

Figure S5.2. Comparison of energetic and entropic barriers to softness calculated using $p_{cut,R} = 0.25$ *and* $p_{cut,R} = 0.125$ *for systems with* $\varepsilon_{AB} = 1.0\ \varepsilon$ *as a function of softness, analogous to Figure 13 in the main text.*